

05,06

Investigation on Structural, Electronic, Thermal, and Thermoelectric Properties of Co_2MnGa under Pressure Based on Density Functional Theory

© A. Fazeli Kisomi¹, S.J. Mousavi², B. Nedae-Shakarab¹

¹ Department of Physics, Ardabil Branch, Islamic Azad University, Ardabil, Iran

² Department of Physics, Rasht Branch, Islamic Azad University, Rasht, Iran

E-mail: alif1364@yahoo.com

Received: May, 5, 2022

Revised: May, 15, 2022

Accepted: May, 16, 2022

Structural, electronic, thermal, and thermoelectric properties of Co_2MnGa under 0, 5, 10, and 15 GPa pressures have been investigated. In electronic properties, in minority spin, a pseudo band gap (about 0.25 eV) is visible. Thermal properties in the range of 0 to 700 K have been calculated. Our results in thermal properties have a good agreement with another theoretical work. Calculations of thermoelectric properties, in both spin up and down, in the range of 100 to 700 K have been done. In spin up, an abnormal behavior is observed under 5 GPa for electrical conductivity. This is due to increase in M_t at this pressure. The sign and value of Seebeck coefficient in spin up at 300 K has a good consistency with experimental work. Other thermoelectric properties such as: power factor, electronic thermal conductivity divided by relaxation time, electronic contribution of heat capacity at constant volume under pressure have been studied.

Keywords: Co_2MnGa , density functional theory, electronic properties under pressure, thermoelectric properties under pressure.

1. Introduction

Heusler compounds are one of the main group in half-metal category compounds that invoke interest among researchers [1–5]. These compounds are divided into two groups: full-Heusler alloys and half-Heusler alloys. Full-Heusler alloys have chemical formula X_2YZ , where X and Y are mostly transition metals and Z is one of the members of groups III–V in periodic table. Structural, electronic, phonon, and magnetic properties of full-Heusler Co-based compounds were investigated by researchers [6–13]. These compounds are promising as good candidates for high-efficiency tunnel magneto-resistance devices [14,15] in spintronic industry. One of the most attractive compounds among them is Co_2MnGa . In experimental works, Webster *et al.* [6] investigated structural and magnetic properties of this alloy such as: lattice constant and total moment magnetization (M_t). Saito and his co-worker [7] studied magnetic and thermoelectric properties of this compound. They found Curie temperature of Co_2MnGa is 700 K. In theoretical studies, Candan *et al.* [8] investigated structural, electronic, phonon, and magnetic properties of this compound under 0 GPa. Mebsout *et al.* [9] calculated thermodynamic properties of this alloy until 18 GPa by code GIBBS [16] and quasi-harmonic Debye model. Ram and his co-workers [17] analyzed structural, magnetic, and electronic properties of Co_2MnGa under various pressures. But theoretical calculations of structural, electronic, and thermoelectric properties of this compound have been neglected at

pressures of less than 20 GPa specially since the value of the Seebeck coefficient at 300 K and under 0 GPa pressure is in a good consistency with experimental work. Also, investigation on thermal properties under these pressures by using new version of GIBBS code, *i.e.*, GIBBS2 [18,19], and Debye–Grüneisen method [19,20] and comparing results with another theoretical work can be attractive.

In this paper, in other sections and subsections, first, we describe computational details that are based on density functional theory. Then, structural properties and after that electronic properties including band structure and total density of states under 0, 5, 10, and 15 GPa pressures have been investigated. In the next step, thermal properties consisting of phonon contribution of heat capacity at constant volume and Debye temperature up to 700 K under mentioned pressures have been studied. In the last subsection of Section 3, thermoelectric properties of Co_2MnGa including Seebeck coefficient, electrical conductivity divided by relaxation time, power factor, electronic thermal conductivity divided by relaxation time, and electronic contribution of heat capacity at constant volume, in both spin up and down in a temperature range of 100 to 700 K under 0, 5, 10, and 15 GPa pressures have been analyzed. In the end of the paper, we conclude our results.

2. Computational details

Our calculations have been done by computational code Wien2k [21] and Full Potential Linear Augmented Plane

Structural properties of Co_2MnGa in present work and other theoretical and experimental works

Pressures	Lattice constant			Bulk modulus		
	Our study, Å	Other theo., Å	Exp., Å	Our study, GPa	Other theo., GPa	Exp., GPa
0 GPa	5.720	5.695 [24], 5.724 [8]	5.77 [6]	190.31	199 [25], 186.7 [8]	–
5 GPa	5.67	–	–	–	–	–
10 GPa	5.62	–	–	–	–	–
15 GPa	5.58	–	–	–	–	–

Waves (FP-LAPW) and accessorial codes GIBBS2 and Boltz Trap [22]. In our calculations with code Wien2k, value of $R_{\text{MT}} \cdot K_{\text{Max}} = 7$, R_{MT} for Co and Mn, 2.23 a.u. and for Ga, 2.1 a.u. have been selected. The number of k-points 3000 and the value of convergence in energy 0.0001 Ry have been considered. GGA(PBE) [23] as an exchange–correlation potential has been used. In our calculations with code GIBBS2, Debye–Grüneisen method is utilized.

3. Results and discussions

3.1. Structural Properties

In Fig. 1, the diagram of energy vs volume for Co_2MnGa has been demonstrated which is fitted by Murnaghan EoS. This compound has a cubic structure $L2_1$ with the Cu_2MnAl -type and $\text{Fm-}3m$ space group. Co_2MnGa has four atoms with atomic positions (0.25, 0.25, 0.25) and (0.75, 0.75, 0.75) for Co, (0.5, 0.5, 0.5) for Mn, and (0, 0, 0) for Ga.

This compound is found to be a ferromagnetic compound with total moment magnetization M_t ($M_t = 4.10 \mu\text{B}$), which has a good consistency with another experimental work ($M_t = 4.05 \mu\text{B}$) [6] and other theoretical works [8,9]. The value of M_t in our calculations under 5 GPa has risen

about $0.01 \mu\text{B}$. But under other pressures it has the values lower than that of under 0 GPa.

In Table, structural properties of Co_2MnGa in present work and other theoretical and experimental works have been listed.

Our results have a good agreement with other experimental and theoretical works. In present work, lattice constants under 5, 10, and 15 GPa pressures have been calculated that are not comparable, because of lacking other similar works. Of course, an increase in pressure leads to a decrease in lattice constant. Also, because of increase in Coulomb interaction, from 10 to 15 GPa, reduction of the lattice constant is lower than under other pressures, which confirms correction of present work.

Strong 3d–3d hybridization of Co and Mn orbitals [9] leads to high bulk modulus for this compound which indicates this compound has a high resistance against pressure and indicates hardness of this compound.

3.2. Electronic properties

Spin-polarized calculations for band structures of Co_2MnGa under pressures 0, 5, 10, and 15 GPa in both majority and minority spin, have been done. The diagrams of band structures for mentioned compound in Fig. 2 in panes *a, c, e*, and *g* for majority spin and in panes *b, d, f*, and *h* for minority spin, have been plotted.

In Co_2MnGa , both majority-spin and minority-spin bands show intersections with the E_F , showing metallic character for both spin channels. This compound in a very small region in minority spin has a pseudo gap in about 0.25 eV which has a good agreement with other theoretical works (0.32 eV [24] and a pseudo gap [8]). This gap is formed due to strong 3d–3d hybridization between the Co and Mn atoms [9]. So we can conclude that Co_2MnGa does not show traditional half-metal behavior. The pseudo-gap value does not change much with increasing pressure up to 15 GPa. This is due to high bulk modulus of this compound and its high resistance against pressure. In contrast of present work, according to Ram *et al.* [17], the gap exceeds 0.3 eV. In comparison between present work and that work, due to better agreement between present work and experimental work [6] (*i.e.*, lattice constant and M_t under 0 GPa), our results are more reliable than [17].

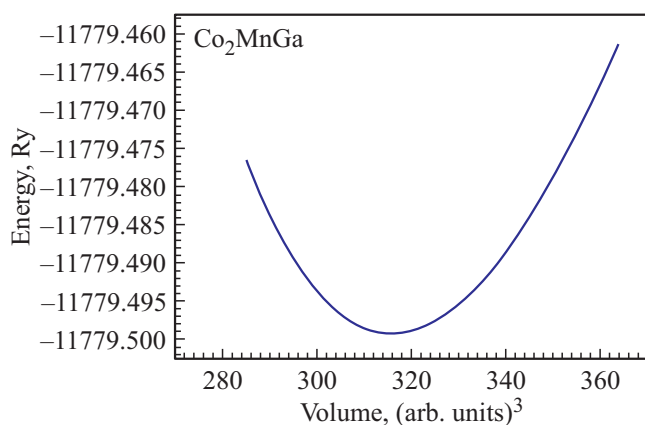


Figure 1. The diagram of energy vs volume for Co_2MnGa which is fitted by Murnaghan EoS.

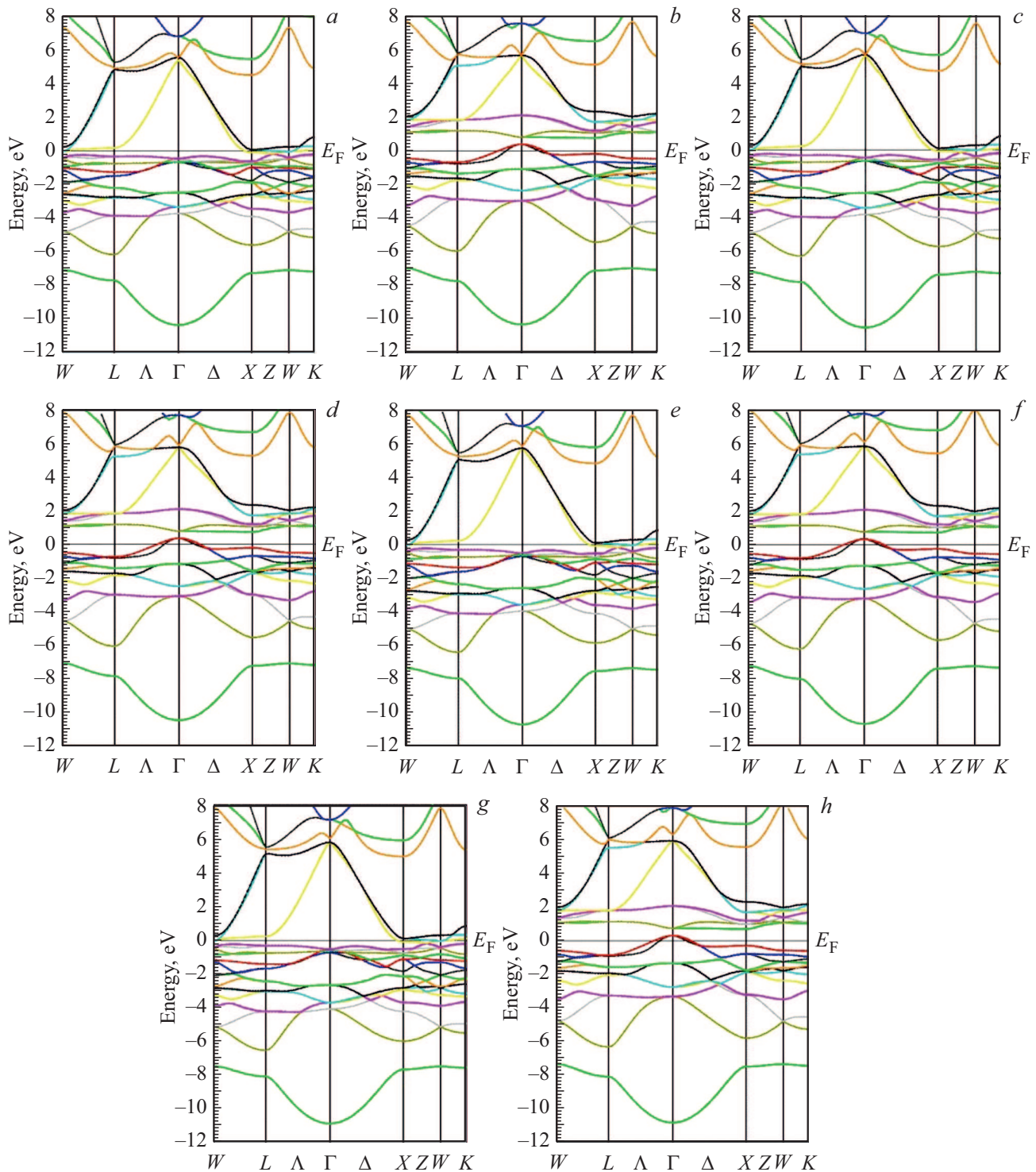


Figure 2. The diagrams of the band structures for majority spin (*a, c, e, g*) and for minority spin (*b, d, f, h*).

The kind of this pseudo gap is direct and is in the direction of Γ , which increase in pressure does not change kind of pseudo gap too. But the increase in pressure causes major changes in the slope of the bands in band structures. These changes are more visible in total DoS diagrams and we saw the effect of these changes on thermoelectric properties.

In Fig. 3, *a* and *b*, the diagrams of total DoS for spin up and spin down under 0, 5, 10, and 15 GPa pressures have been plotted. As is visible, generally, increasing the pressure causes the peaks to move towards more negative energies in valence band while in conduction band move towards more positive energies. These results have a good consistency with another theoretical work about solid under

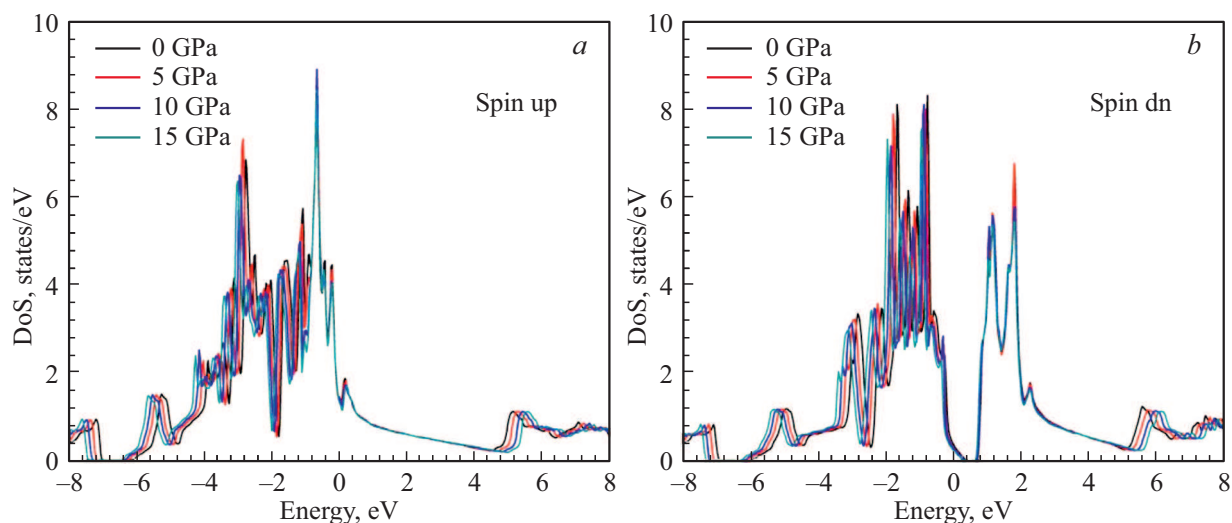


Figure 3. The diagrams of total DoS for *a*) spin up and *b*) spin down.

pressure [26]. This is due to increase the pressure and consequently, abandonment of the equilibrium state of the system and therefore increase in total energy of the system.

In spin up, the sharpest peak belongs to 10 GPa in about -0.6 eV and the second sharpest peak belongs to 5 GPa in about -2.8 eV which indicates more flat bands in band structure in this energy for 5 GPa in comparison with 0, 10, and 15 GPa. This subject is in accord with our calculations for electrical conductivity.

In spin down, the sharpest peaks belong to 0 GPa in valence band and 5 GPa in conduction band. The pseudo gap with value of about 0.25 eV in Fig. 3, *b* is visible, too.

3.3. Thermal properties

In Fig. 4, the diagrams of thermal properties consisting of *a*) phonon contribution of heat capacity at constant volume C_{V-Ph} and *b*) Debye temperature under different pressures until 15 GPa and up to 700 K, *i.e.*, Curie temperature of Co_2MnGa , have been demonstrated. As is visible, the diagram of C_{V-Ph} in all pressures at low temperatures as T^3 -Debye is increased by increasing temperature, while at high temperatures C_{V-Ph} tends to Dulong–Petit limit. Also, an increase in pressure leads to a decrease in the value of C_{V-Ph} . This is due to reduction of the volume and consequently, restriction of phonon oscillations due to increased Coulomb interaction.

However, Debye temperature has a direct relation with sound velocity in compound and is slowly decreasing with increasing temperature, which is due to increased phonon oscillations and reduction of the sound velocity caused by increasing sound scattering. Also, an increase in pressure leads to a rise in Debye temperature, which is due to decreased sound scattering as a result of increase in Coulomb interaction that leads to the restriction of phonon oscillations.

Our calculations have a good consistency with other theoretical work [9]. Phonon contribution of heat capacity at constant volume under 0 GPa pressure and at 300 K temperature in our calculation is $86.002 \text{ J/mol} \cdot \text{K}$ and their result is $84.35 \text{ J/mol} \cdot \text{K}$ that has a good agreement with each other. However, Debye temperature in our calculations under 0 GPa pressure and at 300 K temperature is 525.41 K and in their calculations is 559.67 K which are comparable. Due to more close value of our obtained lattice constant to experimental work, under 0 GPa and at 0 K and considering we used GIBBS2 code (the new version of GIBBS code) and more complete method (Debye–Grüneisen), our study can be more reliable.

3.4. Thermoelectric properties

3.4.1. Thermoelectric properties in spin up

All of the thermoelectric properties in the range of 100 to 700 K temperatures and under 0, 5, 10, and 15 GPa pressures have been calculated.

In Fig. 5, *a*, the diagrams of Seebeck coefficient S vs temperature under various pressures have been plotted. Due to negative sign of the Seebeck coefficient at most of pressures and temperatures, charge carriers are electrons. At most of temperatures, an increase in temperature leads to a rise in the absolute value of Seebeck coefficient. This is because the electrons move faster to the end of solid and create an electrical field against gradient temperature. After 300 K, the absolute value of Seebeck coefficient is reduced by increasing pressure. This is because of electrons velocity reduction due to electrons scattering as a result of reduction in volume and consequently, increase in Coulomb interaction.

Our obtained value for Seebeck coefficient under 0 GPa and at 300 K ($S = -39.64 \mu\text{V/K}$) has a good agreement in comparison with the experimental value [7] ($S = -35.2 \mu\text{V/K}$). However, under 0 GPa and at 600 K

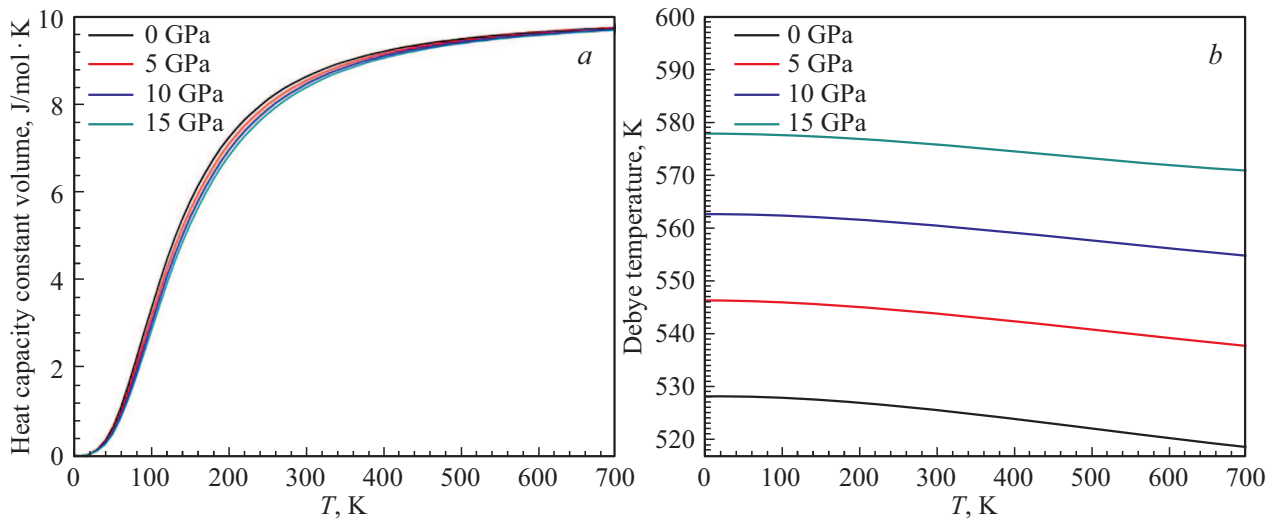


Figure 4. The diagrams of thermal properties consist of a) phonon contribution of heat capacity at constant volume and b) Debye temperature under 0, 5, 10, and 15 GPa pressures up to 700 K.

our obtained value ($S = -59.55 \mu\text{V/K}$) in comparison with another experimental work [7] ($S = -41.2 \mu\text{V/K}$) is acceptable.

In Fig. 5, b, the diagrams of electrical conductivity σ divided by relaxation time τ vs temperature under different pressures have been demonstrated. As it is known, the accessorial code Boltz Trap [22] uses relaxation time approximation and considers σ/τ . As is shown, an increment of temperature leads to an increase in σ/τ . This is for two reasons: reduction in relaxation time and an increase in electrons velocity that leads to an increase in excited electrons. But with increase in pressure, we can see an abnormal behavior under 5 GPa pressure whose diagram lies below the diagram of this parameter under 0 GPa pressure. The reason of this behavior is in an increment of total moment magnetization M_t under 5 GPa that was mentioned in structural properties (Section 3.1). In addition, as in the description of the diagram (Fig. 3, a) is mentioned, the second sharpest peak belongs to 5 GPa. Sharp peak means more flat bands in band structure and heavier effective mass that leads to a reduction in the velocity of electrons. Thus, electrical conductivity is decreased. Under 10 and 15 GPa pressures, by considering the decrease in volume and shorter distance, by which electrons should move for conducting, and that also M_t under both of these pressures is lower than that of 0 GPa, electrical conductivity is increased by rising pressure.

In Fig. 5, c, power factors as $S^2\sigma/\tau$ have been calculated. As is expectable, the diagrams are in order of absolute value of the Seebeck coefficient. This is due to power 2 of S.

In Fig. 5, d, the diagrams of electronic thermal conductivity κ_e divided by relaxation time τ have been plotted. Nothing special is happened by increasing pressure. This means effect of shortening the electrons path due to volume reduction and on the other hand, reduction in electrons velocity affected by increase in Coulomb interaction are

neutralized by each other. According to Wiedmann–Franz law, $\kappa \propto T$. Therefore, an increment of temperature leads to a rise in κ_e , which is due to the increase of the electrons velocity.

In Fig. 5, e, the diagrams of electronic contribution of heat capacity at constant volume CV-el vs temperature under 0, 5, 10, and 15 GPa pressures have been demonstrated. An increase in temperature leads to a rise in electrons oscillations and consequently leads to an increment of CV-el. Because of increase in Coulomb interaction, electrons oscillations are restricted by increasing pressure which leads to a reduction in CV-el.

3.4.2. Thermoelectric properties in spin down

In Fig. 6, a, the diagrams of Seebeck coefficient vs temperature under 0, 5, 10, and 15 GPa pressures have been plotted. The greatest value at 100 K belongs to 0 GPa pressure that had the sharpest peak in total DoS diagram (Fig. 3, b). But increasing the temperature causes the electrons to move faster to reach the end of the solid. This phenomenon and the effect of decrease in volume lead to an increase in the Seebeck coefficient S with raising pressure at high temperatures.

Due to positive sign of S, in most pressures and temperatures charge carriers are holes. An increase in temperature and therefore an increase in excited electrons leads to an increase in the Seebeck coefficient at most of temperatures.

In Fig. 6, b, the diagrams of σ/τ vs temperature under 0, 5, 10, and 15 GPa pressures have been demonstrated. Due to existence of pseudo gap in spin down and constant value of it under pressures and due to increase in Coulomb interaction among electrons affected by reduction of volume, electrical conductivity is decreasing with increasing pressure. Relaxation time is decreasing with increasing temperature and electrons velocity is also increasing with temperature raising. Both of them lead to an increase in σ/τ . On

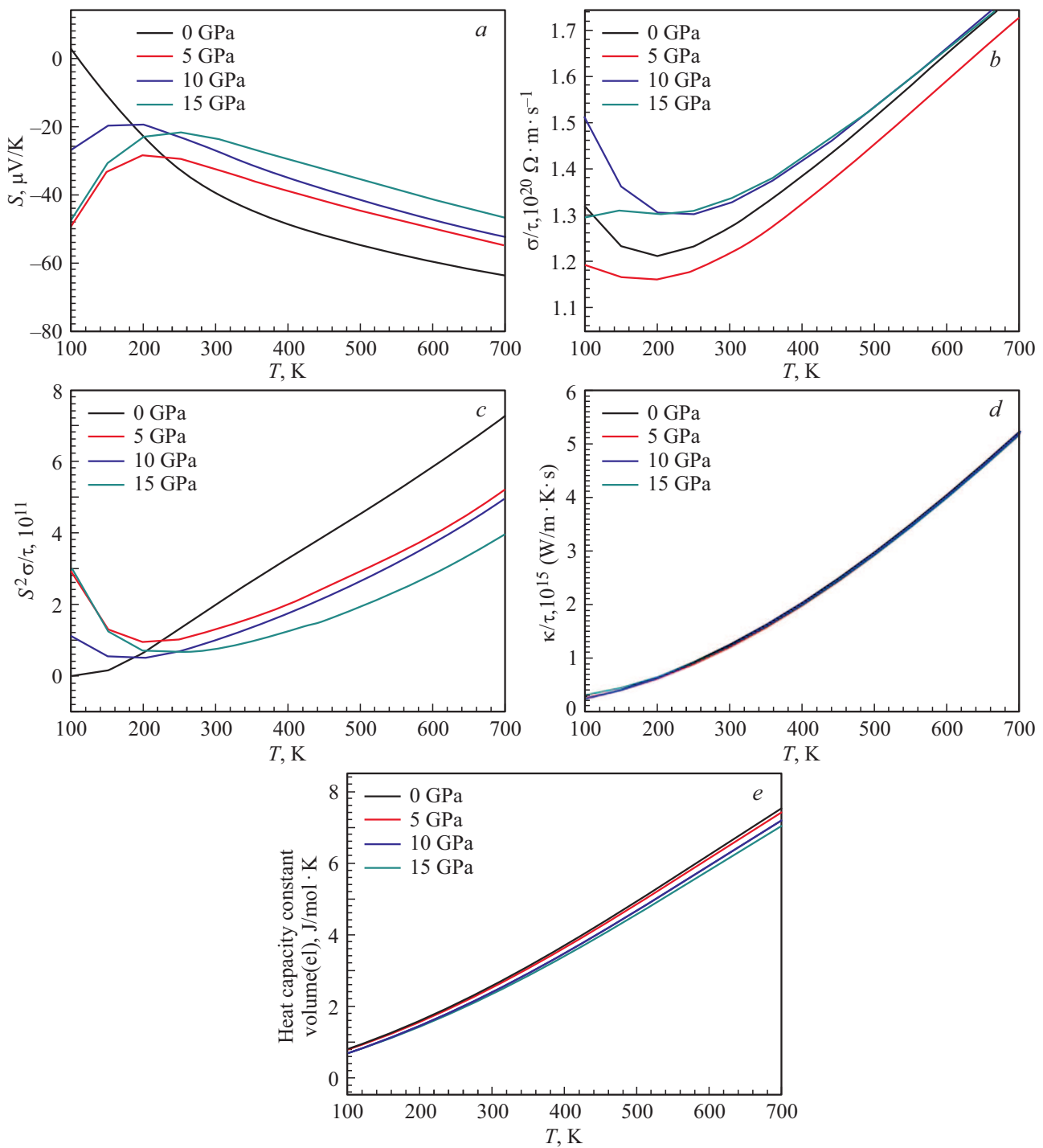


Figure 5. The diagrams of thermoelectric properties include: *a*) Seebeck coefficient S ; *b*) electrical conductivity σ divided by relaxation time τ ; *c*) power factor as $S^2\sigma/\tau$; *d*) electronic thermal conductivity κ_e divided by relaxation time τ ; *e*) electronic contribution of heat capacity at constant volume $C_{V-\text{el}}$, all of them in spin up and in the range of 100 to 700 K temperatures and under 0, 5, 10, and 15 GPa pressures.

the other hand, an increment of temperature leads to increase in phonon–electron interaction and, consequently, reduction in electrical conductivity. Because these factors are neutralized by each other, electrical conductivities after 300 K are approximately straight line or have a slow slope under different pressures.

In Fig. 6, *c*), the diagrams of power factor as $S^2\sigma/\tau$ vs temperature in the range of 100 to 700 K under 0, 5, 10, and 15 GPa pressures have been investigated. The diagrams approximately follow the diagrams of the Seebeck coefficient, except under 5 GPa because of the value of σ/τ lower than that of under 0 GPa. At most temperatures,

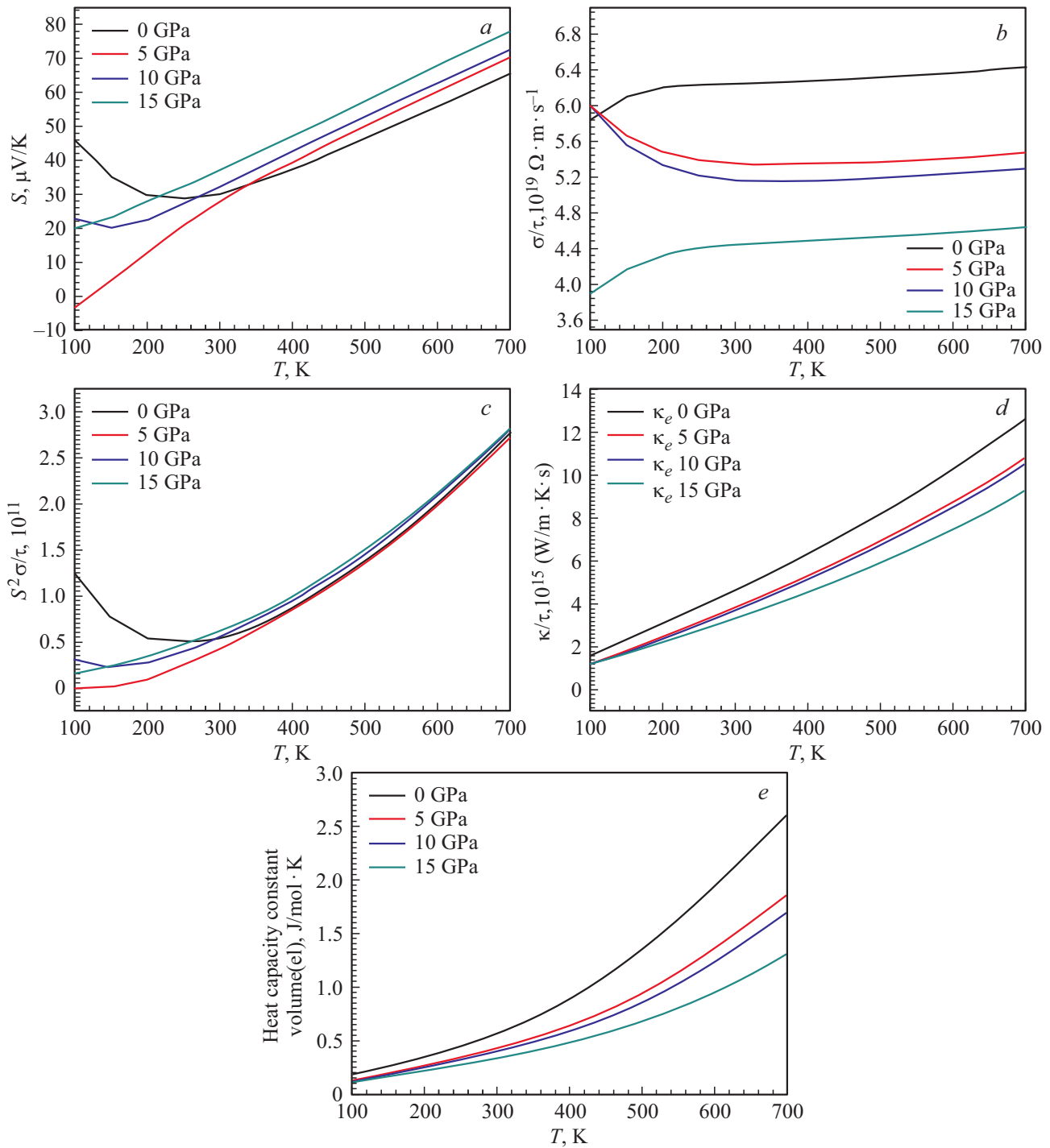


Figure 6. The diagrams of thermoelectric properties include: *a*) Seebeck coefficient S ; *b*) electrical conductivity σ divided by relaxation time τ ; *c*) power factor as $S^2\sigma/\tau$; *d*) electronic thermal conductivity κ_e divided by relaxation time τ ; *e*) electronic contribution of heat capacity at constant volume $C_{V-\text{el}}$, all of them in spin down and in the range of 100 to 700 K temperatures and under 0, 5, 10, and 15 GPa pressures.

power factor like Seebeck coefficient is increasing with increasing pressure. Generally, power factors in both spin up and down are in the range of 10^{11} but their value in the spin up, especially at high temperatures, is higher.

In Fig. 6,*d*, the diagrams of electronic thermal conductivity κ_e divided by relaxation time τ vs temperature

under various pressures have been plotted. According to Wiedmann–Franz law, κ has a direct relation with temperature. Therefore, an increase in temperature leads to a rise in κ_e , while κ_e is decreasing with increasing pressure. This reduction is due to a decrease in volume and an increment of Coulomb interaction.

In Fig. 6, *e*, the diagrams of electronic contribution of heat capacity at constant volume ($C_{V\text{-el}}$) vs temperature under 0, 5, 10, and 15 GPa pressures have been investigated. An increase in temperature leads to a rise in $C_{V\text{-el}}$ because of increase in electrons oscillations. An increase of pressure leads to a reduction of $C_{V\text{-el}}$. This is due to the increased Coulomb interaction and, consequently, restriction of electrons oscillations.

Generally, in thermoelectric properties except in spin up and under 5 GPa pressure, in which an abnormal behavior was observed and this is due to an increase of M_t under 5 GPa pressure in comparison with 0 GPa and lower value of M_t for 10 and 15 GPa than that of 0 GPa. Except this one, no abnormal phenomenon was observed. An increase in pressure up to 5 GPa leads to an increment of M_t in our results. It was seen in Mn_2FeAl compound up to 40 GPa [27].

4. Conclusions

Structural, electronic, thermal, and thermoelectric properties of Co_2MnGa under 0, 5, 10, and 15 GPa pressures have been calculated. Structural properties have a good consistency with other experimental and theoretical works. In minority spin, a pseudo gap of about 0.25 eV has been observed, and other theoretical works confirm correction of our calculations. In thermal properties, an increase of pressure leads to a decrease of $C_{V\text{-ph}}$ while it is increased by raising temperature. On the other hand, Debye temperature is decreasing with increasing temperature, while a rise in pressure leads to an increment of Debye temperature. In thermoelectric properties, power factors in both spin up and down are in the range of 10^{11} but their value in spin up, especially at high temperatures, is higher. κ_e follows Wiedmann–Franz law. Therefore, in both spin up and down, an increase in temperature leads to a rise of κ_e . An increase of pressure leads to a reduction of $C_{V\text{-el}}$, while an increase of temperature leads to an increment of $C_{V\text{-el}}$.

Conflicts of interests

The authors declare that they have no conflict of interest.

References

- [1] E.G. Ozdemir and Z. Merdan. *J. Alloys. Compd.* **807**, 18, 151656 (2019).
- [2] H. Abbassa, A. Labdelli, S. Meskine, Y. Benaissa Cherif, and A. Boukortt. *Mod. Phys. Lett. B* **34**, 2, 2050028 (2020).
- [3] F. Lei, C. Tang, S. Wang, and W. He. *J. Alloys. Compd.* **509**, 17, 5187 (2011).
- [4] A. Bentouaf, F. Bouras, R. Mebsout, and B. Aissa. *J. Supercond. Nov. Magn.* **33**, 4, 1177 (2020).
- [5] A. Anjami, A. Boochani, S.M. Elahi, and H. Akbari. *Results Phys.* **7**, 3522 (2017).
- [6] P.J. Webster. *J. Phys. Chem. Solids* **32**, 6, 1221 (1971).
- [7] T. Saito and D. Nishio-Hamane. *Physica B* **603**, 412761 (2021).
- [8] A. Candan, G. Ugur, Z. Charifi, H. Baaziz, and M.R. Ellialtioglu. *J. Alloys. Compd.* **560**, 215 (2013).
- [9] R. Mebsout, S. Amari, S. Mecabih, B. Abbar, and B. Bouhafis. *Int. J. Thermophys.* **34**, 3, 507 (2013).
- [10] S. Picozzi, A. Continenza, and A.J. Freeman. *Phys. Rev. B* **66**, 9, 94421 (2002).
- [11] S. Ouardi, G.H. Fecher, B. Balke, A. Beleanu, X. Kozina, G. Stryganyuk, C. Felser, W. Klob, H. Schrader, F. Bernardi, J. Morais, E. Ikenaga, Y. Yamashita, S. Ueda, and K. Kobayashi. *Phys. Rev. B* **84**, 15, 155122 (2011).
- [12] H. Joshi, D.P. Rai, Sandeep, and R.K. Thapa. *J. Phys. Conf. Ser.* **765**, 012010 (2016).
- [13] S. Amari, R. Mebsout, S. Mécabih, B. Abbar, and B. Bouhafis. *Intermetallics* **44**, 26 (2014).
- [14] S. Ishida, S. Fujii, S. Kashiwagi, and S. Asano. *J. Phys. Soc. Jpn* **64**, 2152 (1995).
- [15] S. Ishida, T. Masaki, S. Fujii, and S. Asano. *Physica B* **245**, 1-2, 1 (1998).
- [16] M.A. Blanco, E. Francisco, and V. Luaña. *Comput. Phys. Commun.* **158**, 1, 57 (2004).
- [17] S. Ram, M.R. Chauhan, K. Agarwal, and V. Kanchana. *Philos. Mag. Lett.* **91**, 8, 545 (2011).
- [18] A. Otero-de-la-Roza and V. Luaña. *Comput. Phys. Commun.* **182**, 8, 1708 (2011).
- [19] A. Otero-de-la-Roza, D. Abbasi-Pérez, and V. Luaña. *Comput. Phys. Commun.* **182**, 10, 2232 (2011).
- [20] A. Fazeli Kisomi and S.J. Mousavi. *Mater. Phys. Mech.* **40**, 1, 112 (2018).
- [21] P. Blaha, G.K.H. Madsen, D. Kvasnicka, and J. Luitz. WIEN2K, an Augmented Plane Wave Plus Local Orbitals Program for Calculating Crystal Properties. Vienna, Austria (2008).
- [22] G.K.H. Madsen and D.J. Singh. *Comput. Phys. Commun.* **175**, 1, 67 (2006).
- [23] J.P. Perdew, K. Burke, and M. Ernzerhoff. *Phys. Rev. Lett.* **77**, 18, 3865 (1996).
- [24] R.A. Faregh, A. Boochani, S.R. Masharian, and F.H. Jafarpour. *Int. Nano. Lett.* **9**, 339 (2019).
- [25] A. Ayuela, J. Enkovaara, K. Ullakko, and R.M. Nieminen. *J. Phys.: Condens. Matter* **11**, 8, 2017 (1999).
- [26] A. Fazeli Kisomi, B. Nedae-Shakarab, A. Boochani, H. Akbari, and S.J. Mousavi. *Phys. Solid State.* **61**, 11, 1969 (2019).
- [27] Z.-J. Yang, Q.-H. Gao, H.-N. Xiong, J.-X. Shao, X.-W. Wang, and Z.-J. Xu. *Sci. Rep.* **7**, 16522 (2017).